General Disclaimer

- This document has been reproduced from the best copy furnished by the organizational source. It is being released in the interest of making available as much information as possible.

- This document may contain data, which exceeds the sheet parameters. It was furnished in this condition by the organizational source and is the best copy available.

- This document may contain tone-on-tone or color graphs, charts and/or pictures, which have been reproduced in black and white.

- This document is paginated as submitted by the original source.

- Portions of this document are not fully legible due to the historical nature of some of the material. However, it is the best reproduction available from the original submission.

DEPARTMENT OF MECHANICAL ENGINEERING AND MECHANICS
SCHOOL OF ENGINEERING
OLD DOMINION UNIVERSITY
NORFOLK, VIRGINIA

A SECOND-ORDER ACCURATE PARABOLIZED NAVIER-STOKES ALGORITHM FOR INTERNAL FLOWS

By

Tawit Chitsomboon

and

S. N. Tiwari, Principal Investigator

Progress Report
For the period ending July 31, 1984

Prepared for the
National Aeronautics and Space Administration
Langley Research Center
Hampton, Virginia 23665

Under
Research Grant NAG-1-423
Dr. Ajay Kumar, Technical Monitor
HSAD-Computational Methods Branch

November 1984

DEPARTMENT OF MECHANICAL ENGINEERING AND MECHANICS
SCHOOL OF ENGINEERING
OLD DOMINION UNIVERSITY
NORFOLK, VIRGINIA

A SECOND-ORDER ACCURATE PARABOLIZED NAVIER-STOKES ALGORITHM FOR INTERNAL FLOWS

By

Tawit Chitsomboon

and

S. N. Tiwari, Principal Investigator

Progress Report
For the period ending July 31, 1984

Prepared for the
National Aeronautics and Space Administration
Langley Research Center
Hampton, Virginia 23665

Under
Research Grant NAG-1-423
Dr. Ajay Kumar, Technical Monitor
HSAD-Computational Methods Branch

Submitted by the
Old Dominion University Research Foundation
P.O. Box 6369
Norfolk, Virginia 23508

November 1984

FOREWORD

This report covers the work completed on the research project "Analysis and Computation of Internal Flow Field in a Scramjet Engine." The work was supported by the NASA Langley Research Center (Computational Methods Branch of the High-Speed Aerodynamics Division) through research grant NAG-1-423, and monitored by Dr. Ajay Kumar of the High-Speed Aerodynamics Division.

TABLE OF CONTENTS

	Page
FOREWORD	ii
SUMMARY	1
1. INTRODUCTION	1
2. THE PNS EQUATIONS FOR TWO-DIMENSIONAL FLOW	2
3. FINITE-DIFFERENCE ALGORITHM	4
4. NUMERICAL SMOOTHING	5
5. RESULTS AND DISCUSSION	6
5.1 Inviscid Flow with an Incident Shock Wave on a Flat Plate	6
5.2 Inviscid Internal Flow Over a 10-Degree Wedge, $M_\infty = 5$	10
5.3 Viscous Internal Flow Over a 10-Degree Wedge, $M_\infty = 5$	10
6. CONCLUSIONS	18
REFERENCES	20

LIST OF FIGURES

Figure		Page
5.1	Schematic diagram for inviscid supersonic flow over a flat plate	7
5.2	Pressure contours for the initial conditions of Figure 1	8
5.3	Surface pressure distribution for supersonic flow over a flate plate	9
5.4	Pressure distribution at 1/4 inch from the solid wall for supersonic flow over a flate plate	11
5.5	Geometry of the internal flow over a 10-degree wedge	12

TABLE OF CONTENTS - Concluded

LIST OF FIGURES - Concluded

Figure		Page
5.6	Pressure contours for the inviscid internal flow over a 10-degree wedge, $M_\infty = 5$	13
5.7	Surface pressure distribution for the inviscid internal flow over a 10-degree wedge, $M_\infty = 5$	14
5.8	Pressure distribution at 2 cm. from the solid wall for the inviscid internal flow over a 10-degree wedge, $M_\infty = 5$	15
5.9	Pressure contours for the viscous internal flow over a 10-degree wedge, $M_\infty = 5$	16
5.10	Surface pressure distribution for the viscous internal flow over a 10-degree wedge, $M_\infty = 5$	17
5.11	Pressure distribution at 2 cm. from the solid wall for the viscous internal flow over a 10-degree wedge, $M_\infty = 5$	18

A SECOND-ORDER ACCURATE PARABOLIZED NAVIER-STOKES ALGORITHM FOR INTERNAL FLOWS

By

Tawit Chitsomboon[1] and S. N. Tiwari[2]

SUMMARY

A parabolized Navier-Stokes algorithm is presented which is implicit and of second-order accuracy in both the cross flow and marching directions. The algorithm is used to analyze three model supersonic flow problems (the flow over a flat plate with an impinging shock, and inviscid and viscous flows over a 10-degree wedge). The results are found to be in good agreement with the results of other techniques available in the literature.

1. INTRODUCTION

Parabolized Navier-Stokes (PNS) equations have recently become popular in solving steady supersonic flows. The increase in the use of the PNS equations is due to the fact that the algorithm is very efficient with regard to both execution times and storage requirements.

Unlike boundary-layer type equations, the PNS equations allow cross-stream interaction because the normal momentum equation is retained. Reversal of the flow field in the streamwise direction, however, is not permitted because the parabolic nature of the equations dictates no upstream influence.

In order for the code described in this report to be applicable, the flow field must be supersonic. A small fraction of a subsonic layer close

[1]Graduate Research Assistant, Department of Mechanical Engineering and Mechanics, Old Dominion University, Norfolk, Virginia 23508.
[2]Eminent Professor, Department of Mechanical Engineering and Mechanics, Old Dominion University, Norfolk, Virginia 23508.

to solid walls is permitted, but the layer must not be too big as to dominate the entire flow field. These conditions usually are satisfied for high Reynolds number supersonic flows over bodies of small geometrical variations in the streamwise direction.

The algorithm presented in this study is implicit and of second-order accuracy in both cross flow and marching directions. The generalized transformation of coordinates is used for convenience of boundary-conditions implementation. The algorithm is used to analyze a model two-dimensional, supersonic inlet problem at high Mach number and a supersonic flow over a flat plate with an incident shock wave. The results of these model problems are compared with the results of other techniques.

2. THE PNS EQUATIONS FOR TWO-DIMENSIONAL FLOW

The governing equations for the present study are presented here briefly. For a descriptive representation of both two- and three-dimensional equations, reference should be made to Refs. 1 and 2.

The Navier-Stokes equations for a steady two-dimensional flow without body forces and internal heat generation can be written in a non-dimensional conservation-law form (for a Cartesian coordinates system) as

$$\frac{\partial}{\partial x}(E - E_v) + \frac{\partial}{\partial y}(F - F_v) = 0 \qquad (2.1)$$

where

$$E = \begin{bmatrix} \rho u \\ \rho u^2 + p \\ \rho uv \\ (\rho e_t + p)\, u \end{bmatrix} \quad ; \quad E_v = \begin{bmatrix} 0 \\ \tau_{xx} \\ \tau_{xy} \\ u\tau_{xx} + v\tau_{xy} + q_x \end{bmatrix}$$

$$F = \begin{bmatrix} \rho v \\ \rho uv \\ \rho v^2+p \\ (\rho e_t+p)v \end{bmatrix} \quad ; \quad F_v = \begin{bmatrix} 0 \\ \tau_{xy} \\ \tau_{yy} \\ u\tau_{xy}+v\tau_{yy}+q_y \end{bmatrix}$$

To close the system of equations, the following perfect gas equation of state is used.

$$p = (\gamma - 1)\, \rho e \tag{2.2}$$

The coefficient of viscosity is determined from Sutherland's model.

Next, equation (2.1) is transformed into the body-conforming coordinates and put into a strong conservation-law form as follows:

$$\frac{\partial}{\partial \xi} (\bar{E}) + \frac{\partial}{\partial \eta} (\bar{F}) = 0 \tag{2.3}$$

where

$$\bar{E} = \frac{1}{J} [\xi_x E + \xi_y F]$$

$$\bar{F} = \frac{1}{J} [\eta_x (E - E_v) + \eta_y (F - F_v)]$$

and J represents the Jacobian of transformation, and ξ_x, ξ_y, η_x, η_y are the metrics of transformation. In order to put equation (2.3) in the PNS form all the viscous cross-derivative terms in $\bar{F}$ have been neglected.

Unless properly treated, the streamwise pressure gradient in the subsonic layer will cause the marching procedure to be divergent. In this

study, Vigneron's technique, in which only a fraction of the streamwise pressure gradient is retained (Ref. 2), is used as opposed to the sublayer approximation employed in Refs. 1 and 5.

The modified equation suitable for a stable marching is then expressed as:

$$\frac{\partial \bar{E}^*}{\partial \xi} + \frac{\partial \bar{P}}{\partial \xi} + \frac{\partial \bar{F}}{\partial \eta} = 0 \qquad (2.4)$$

$$\bar{E}^* = \bar{E} - \bar{P}$$

$$\bar{P} = \frac{1}{J}\left[0,\ (1-w)\,\xi_x P,\ (1-w)\,\xi_y P,\ 0\right]^T$$

where w is a parameter obtained from an eigenvalue analysis (Ref. 2).

3. FINITE-DIFFERENCE ALGORITHM

A fully implicit, non-iterative, finite-difference algorithm, as described by Schniff and Steger (Ref. 1), is employed in this study. The resulting algorithm is in delta form and requires a block-tridiagonal inversion at each marching step. The details of the algorithm are available in Ref. 1 and the final form is expressed here as:

$$\left[\tilde{A}^i + (1-\alpha)\,\Delta\,\xi\,\delta_\eta\,\tilde{B}^i\right]\Delta^i q =$$

$$-\left(\tilde{A}^i - \tilde{A}^{i-1}\right) q^i + \alpha\left(\bar{E}^{*i} - \bar{E}^{*i-1}\right)$$

$$-(1-\alpha)\,\Delta\xi\delta_\eta\,\tilde{\bar{F}}^i - \Delta^{i-1}\bar{P} \qquad (3.1)$$

In equation (3.1) if $\alpha = 0$ the algorithm is first-order accurate and if $\alpha = 1/3$ it is second-order accurate. The quantities $\tilde{A}$ and $\tilde{B}$ are the Jacobian matrices resulting from the linearization of $\bar{E}$ and $\bar{F}$ with respect to q, respectively; they are 4x4 matrices for the two-dimensional case. The tildes above A, B and $\bar{F}$ indicate that the metric coefficients are to be evaluated at the station (i+1), whereas the Jacobian of transformation is evaluated at the i^{th} station.

For the viscous case, the boundary conditions are two no-slip conditions, zero normal pressure gradient, and a specified temperature at the solid wall. The method of simple extrapolations has been used successfully to implement the boundary conditions for the inviscid cases. For this method to work well, it is necessary to cluster the grid points near the solid wall.

With an appropriate initial data plane, the PNS algorithm of equation (3.1) can be marched in the ξ direction in one sweep to obtain a solution. Because this is an implicit scheme, the solution procedure requires an inversion of a block-tridiagonal system.

4. NUMERICAL SMOOTHING

For viscous as well as inviscid marching, both implicit and explicit smoothing terms of second and fourth order, respectively, are employed to dampen the oscillation. The implicit smoothing function also serves to make the diagonal terms of the block-tridiagonal system non-zero.

By numerical experiments, it is found that smoothing functions on q vector are more effective than smoothing functions on the flux vector $\bar{E}$ which is used in Refs. 1 and 5.

The second-order implicit smoothing term of the form

$$-\frac{\varepsilon_I}{J^{i+1}}(\nabla\Delta)\, J^{i+1}\, q^{i+1}$$

is added to the left-hand side of equation (3.1), whereas the fourth-order explicit smoothing term is implemented as

$$-\frac{\varepsilon_E}{J^{i}}(\nabla\Delta)^2\, J^{i}\, q^{i}$$

and is added to the right-hand side of equation (3.1).

From linear stability analysis, the upper-bound value of ε_E is 1/8. For the present model problems, the explicit smoothing function alone cannot stabilize the marching procedure. The marching will be stable if the value of ε_I is bigger than a value which is proportional to the step size. This value of ε_I has to be determined numerically. It is found also that if the value of ε_I is two to three times that of ε_E, the upper-bound value of ε_E is not restricted.

5. RESULTS AND DISCUSSION

Three test cases have been run to test the PNS algorithm. A brief discussion of the results is presented here.

5.1 Inviscid Flow with an Incident Shock Wave on a Flate Plate

The schematic diagram for this case is illustrated in Figure 5.1. The initial data plane was obtained from the exact solution of a Mach-2.9 flow over an 11-degree wedge.

A pressure-contour plot of the solution is shown in Figure 5.2. Figure 5.3 compares the normalized surface pressure on the flate plate with the

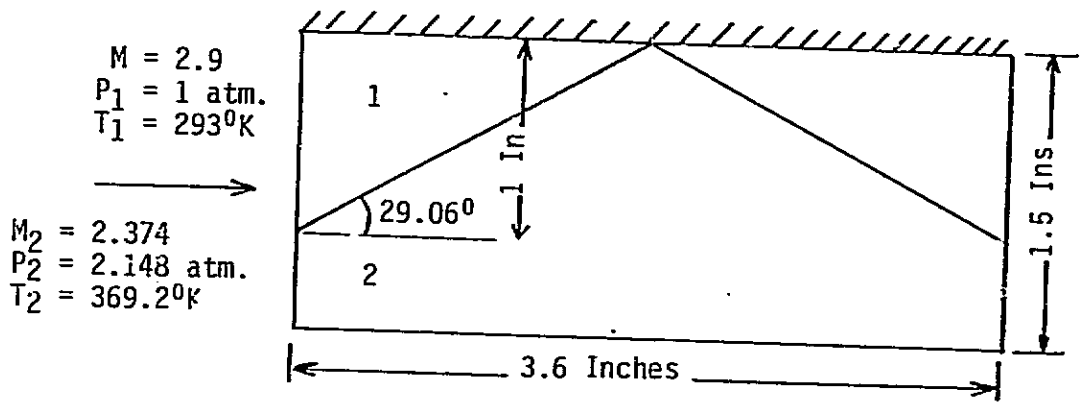

Figure 5.1. Schematic diagram for inviscid supersonic flow over a flat plate.

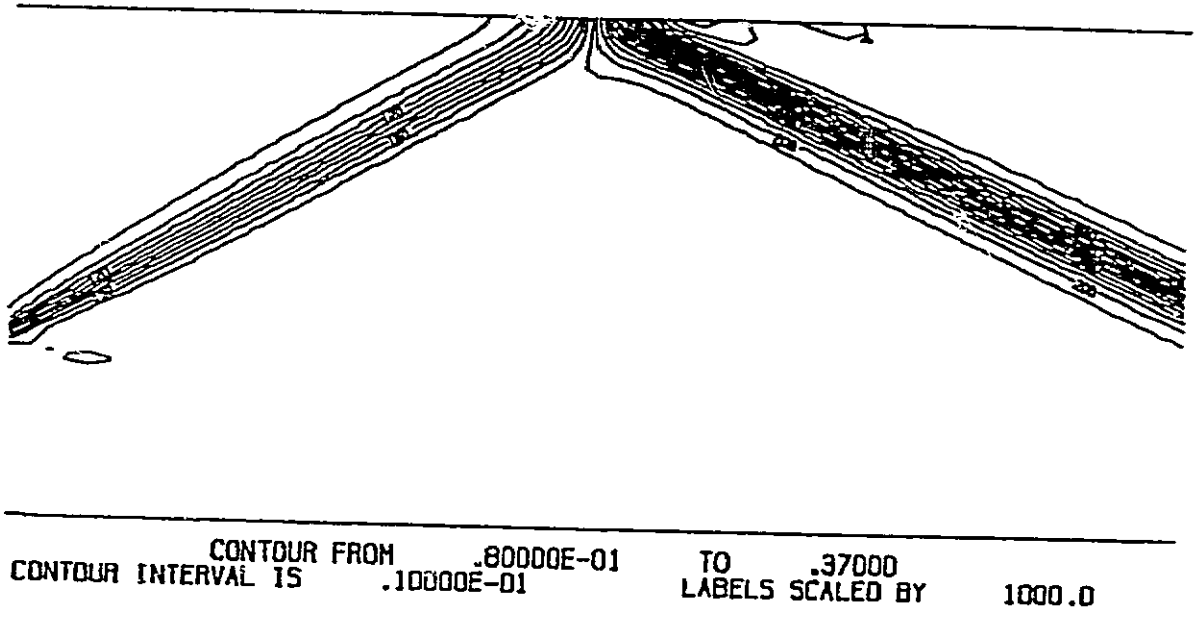

Figure 5.2. Pressure contours for the initial conditions of Figure 1.

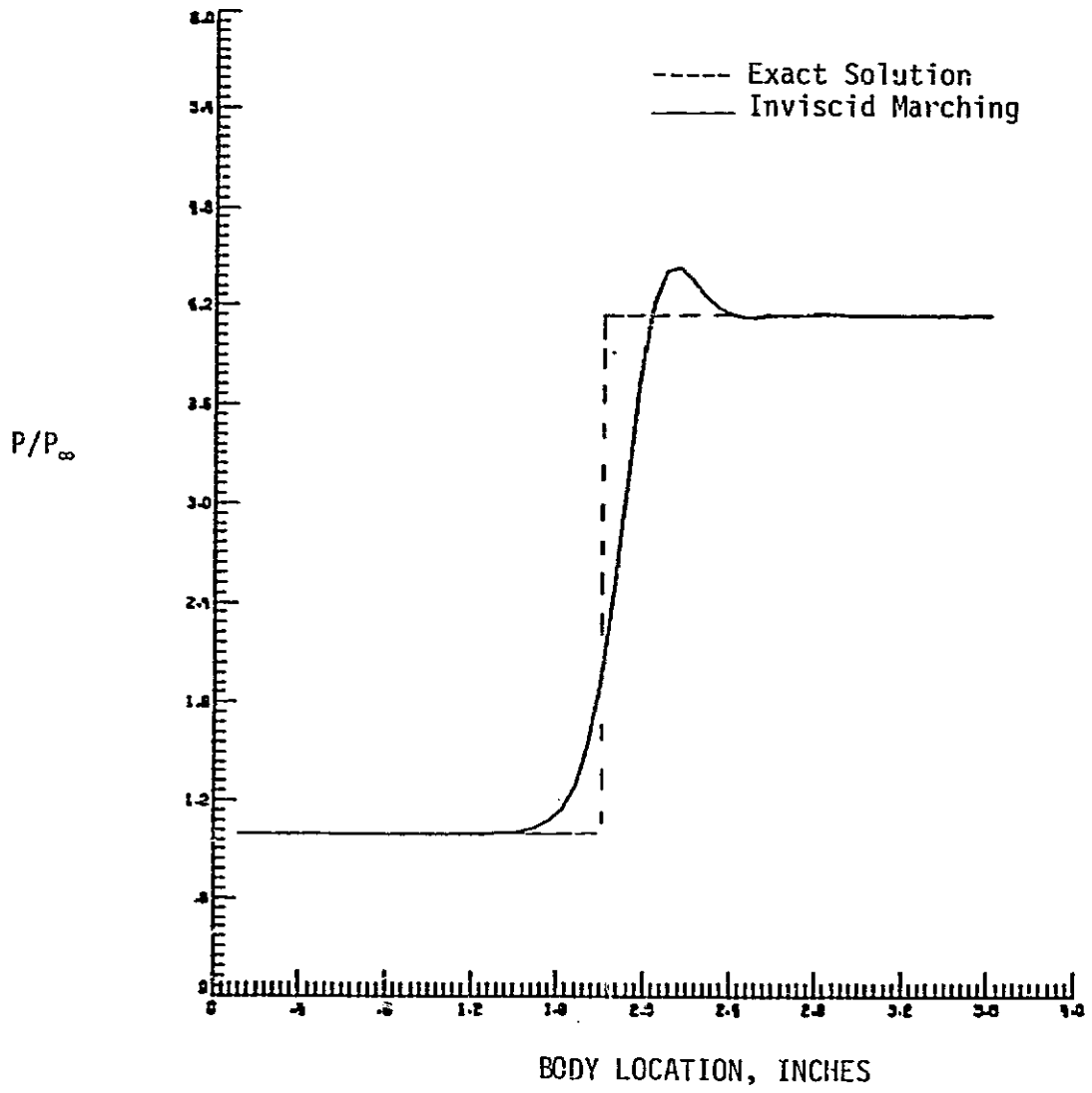

Figure 5.3. Surface pressure distribution for supersonic flow over a flate plate.

exact solution obtained from a shock table. The pressure at 1/4 inch from the plate is compared with the MacCormack's predictor-corrector method and Osher's flux-splitting method in Figure 5.4. The results are seen to be in very good agreement with the results of other techniques.

5.2 Inviscid Internal Flow Over a 10-Degree Wedge, $M_\infty = 5$

The geometry and free stream conditions of this case are shown in Figure 5.5. The initial data plane for this case is specified as a uniform flow of free-stream conditions at 1 cm. from the wedge.

Figure 5.6 shows a pressure-contour plot of the solution. The results for surface-pressure distribution shown in Figure 5.7 indicate a very good agreement with the results of MacCormack's method of Ref. 3. The pressure distribution at 2 cm. from the solid wall is compared with that of Ref. 3, using the MacCormack's method, in Figure 5.8. It is seen that the peak pressure of the inviscid-marching solution is delayed downstream by almost 1 cm. More investigations are needed to improve the agreement. The oscillation after the peak pressure for the MacCormack solution is non-physical and is due to the grid-size aspect ratio.

5.3 Viscous Internal Flow Over a 10-Degree Wedge, $M_\infty = 5$

The geometry and free-stream conditions of this case are the same as for the inviscid case. The initial data plane is specified at 1 cm. from the wedge and is obtained from the solution of Ref. 3.

The pressure-contour plot in Figure 5.9 shows a splitting of the shock wave; this is due to the oscillation across the shock wave. Figure 5.10 indicates a fairly good agreement in the surface pressure with the full Navier-Stokes solution of Ref. 3. The pressure at 2 cm. from the wall is compared with that of Ref. 3 in Figure 5.11. As in the inviscid case, the peak pressure is seen to be delayed in the downstream region.

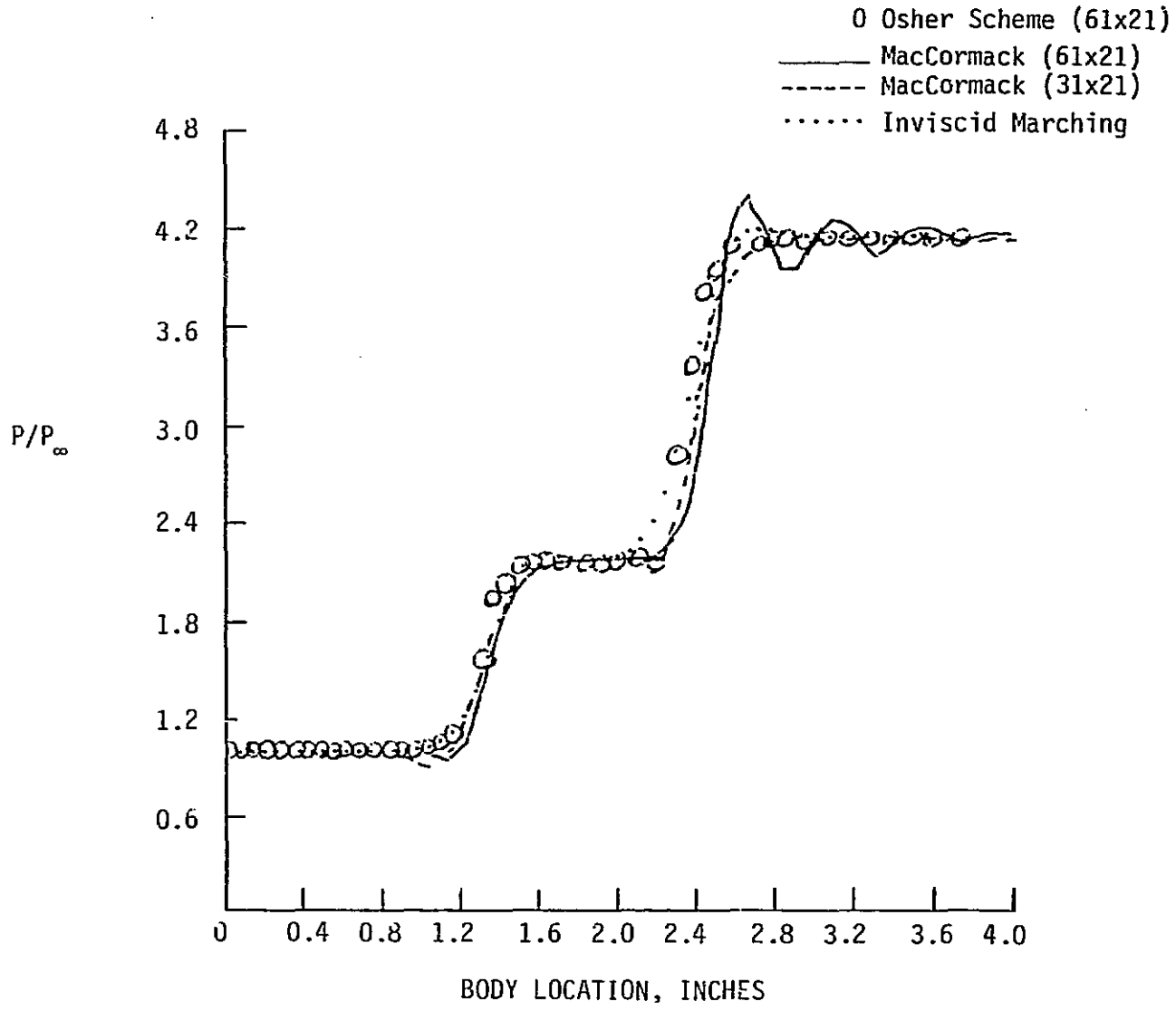

Figure 5.4. Pressure distribution at 1/4 inch from the solid wall for supersonic flow over a flat plate.

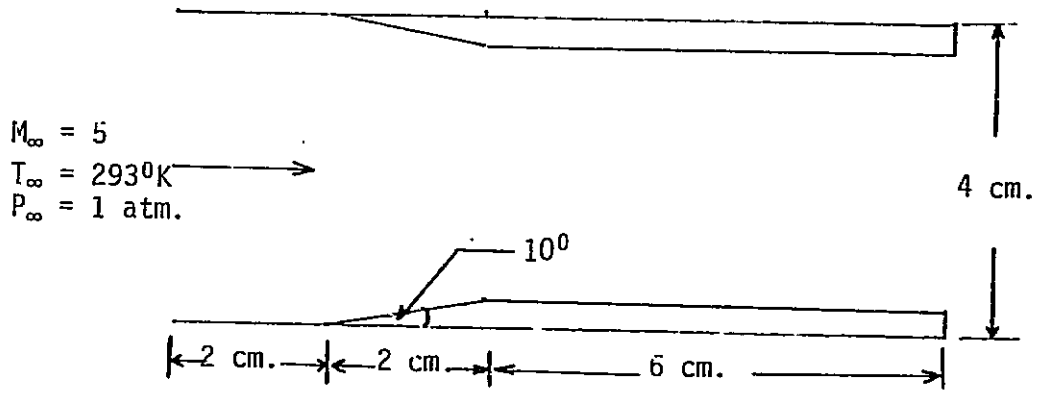

Figure 5.5. Geometry of the internal flow over a 10-degree wedge.

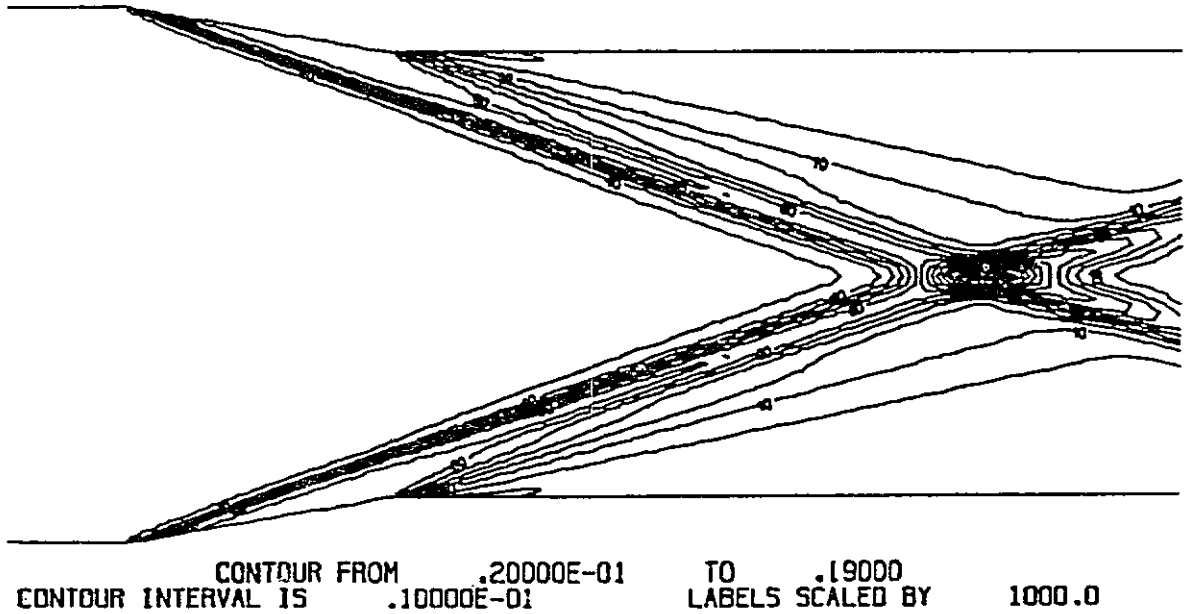

Figure 5.6. Pressure contours for the inviscid internal flow over a 10-degree wedge, $M_\infty = 5$.

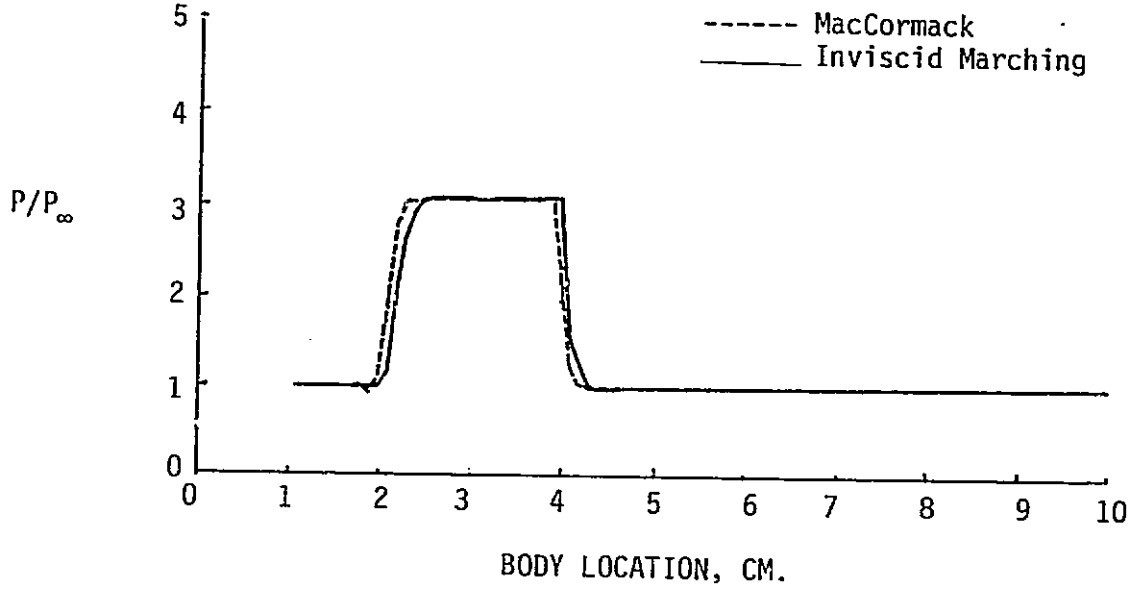

Figure 5.7. Surface pressure distribution for the inviscid internal flow over a 10-degree wedge, $M_\infty = 5$.

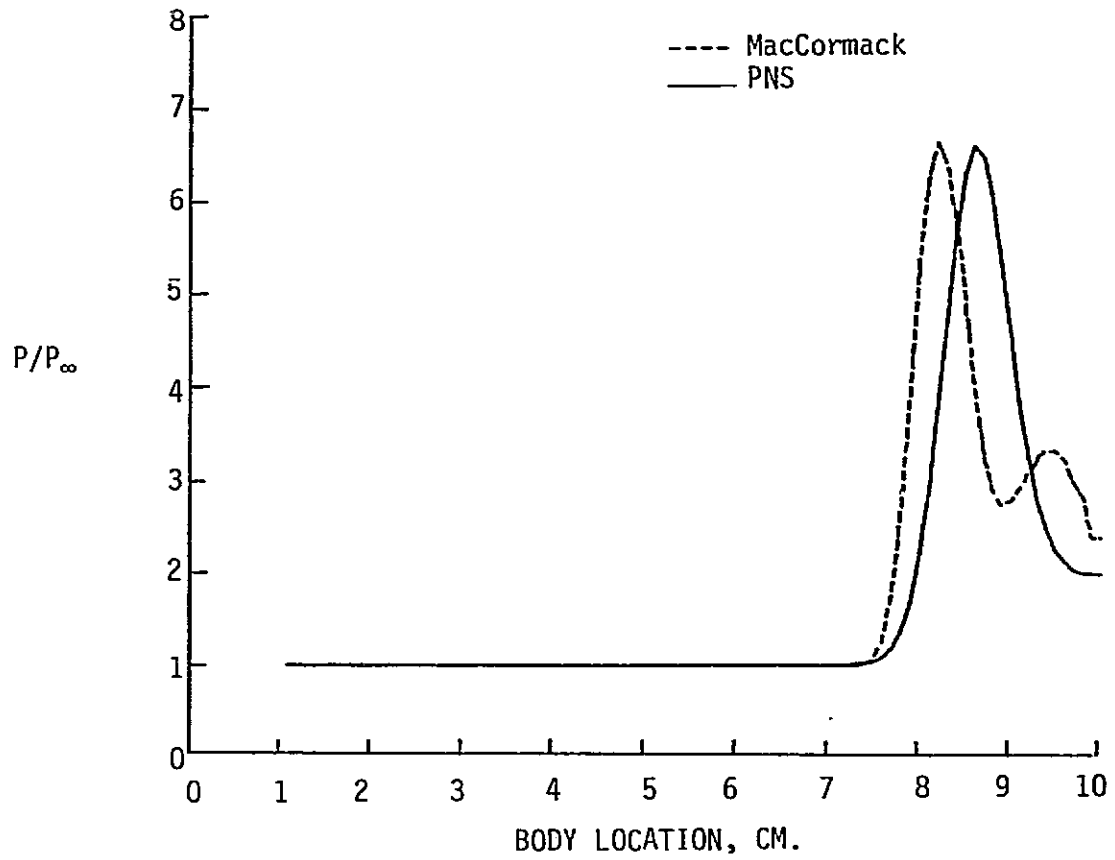

Figure 5.8. Pressure distribution at 2 cm. from the solid wall for the inviscid internal flow over a 10-degree wedge, $M_\infty = 5$.

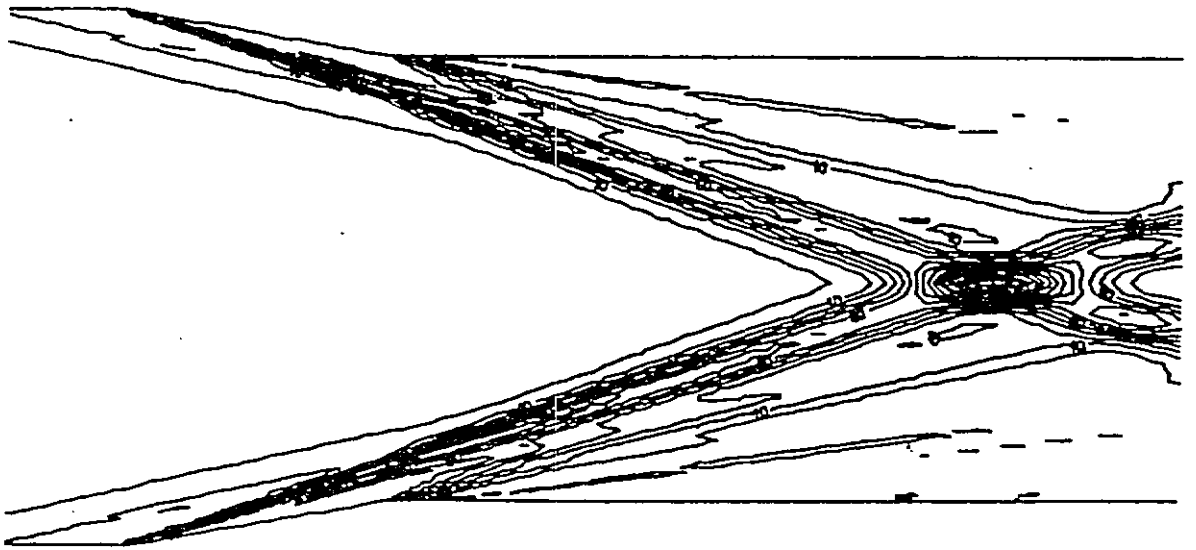

Figure 5.9. Pressure contours for the viscous internal flow over a 10-degree wedge, $M_\infty = 5$.

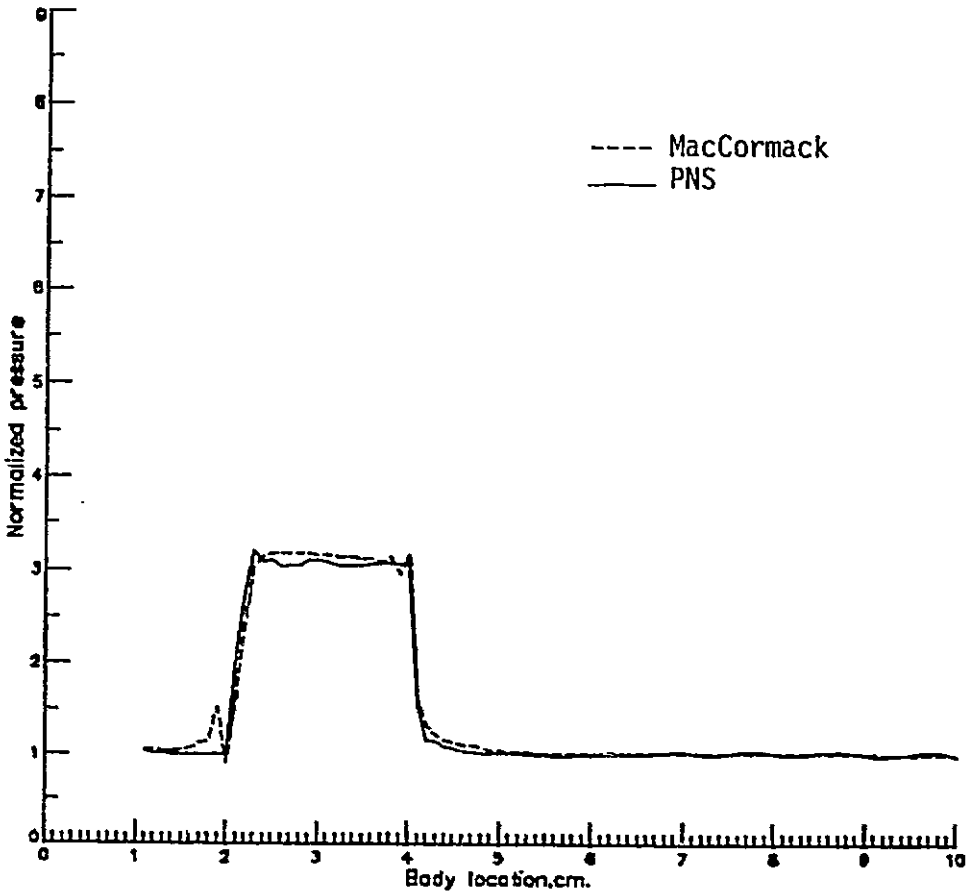

Figure 5.10. Surface pressure distribution for the viscous internal flow over a 10-degree wedge, $M_\infty = 5$.

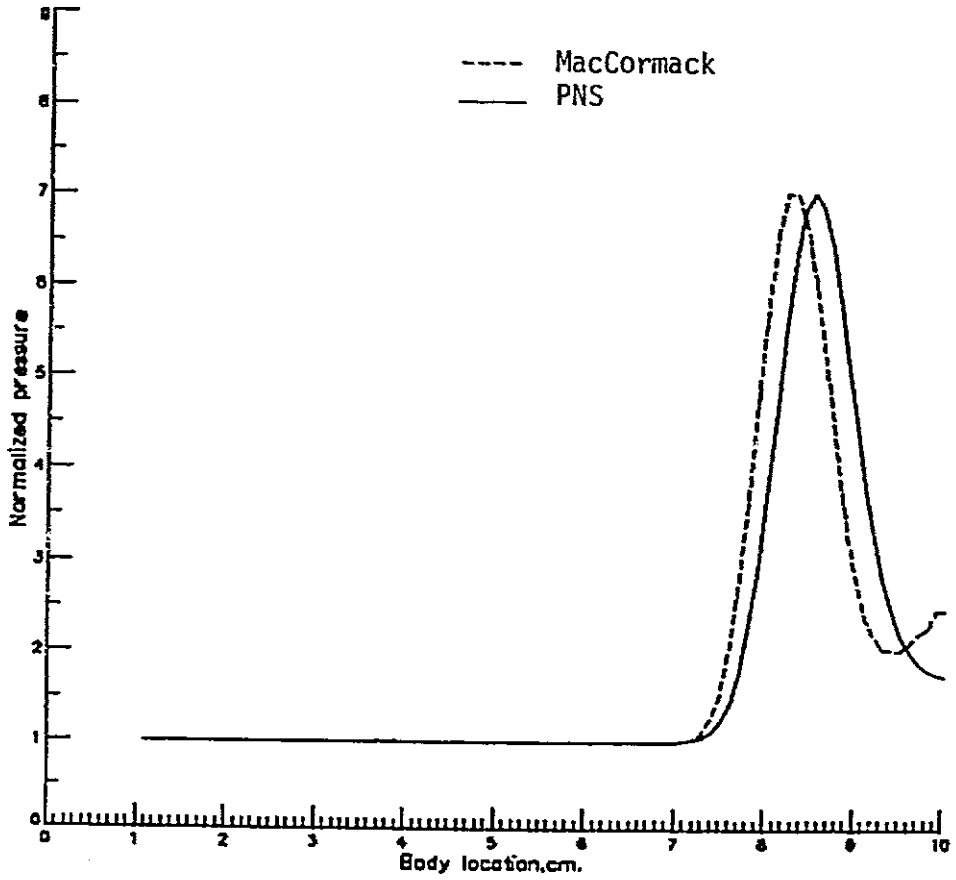

Figure 5.11. Pressure distribution at 2 cm. from the solid wall for the viscous internal flow over a 10-degree wedge, $M_\infty = 5$.

6. CONCLUSIONS

The second-order PNS algorithm due to Schiff and Steger (Ref. 1) has been coded and run successfully for three model problems. Good results are obtained for the flow over a flat plate with an impinging shock wave. Solutions of the flows over a 10-degree wedge indicate the difference in the peak pressure locations. This difference is believed to be due to the splitting of the shock waves which, in turn, is caused by oscillations of the solutions. Investigations are being made to improve the peak pressure locations.

Also, the formulation of a fairly general second-order marching algorithm is under current investigation. This algorithm will not be restricted to only a three-point-backward differencing scheme of Ref. 1. The results obtained from this general algorithm will be compared with other PNS codes as well as with the full Navier-Stokes solutions.

REFERENCES

1. Schiff, L.B. and Steger, J.L., "Numerical Simulation of Steady Supersonic Viscous Flow," AIAA Paper 79-0130, January 1979.

2. Vigneron, Y.C., Rakich, J.V., and Tannehill, J.C., "Calculation of Supersonic Viscous Flow Over a Delta Wing with Sharp Subsonic Leading Edge," AIAA Paper 78-1137, July 1978.

3. Kumar, A., "Some Observations on a New Numerical Method for Solving the Navier-Stokes Equations," NASA TP-1940, November 1981.

4. Venkatapathy, E., Rakich, J.V., and Tannehill, J.C., "Numerical Solution of Space Shuttle Orbiter Flow Field," AIAA Paper 82-0028, January 1982.

5. Srinivasan, G.R. and Nicolet, W.E., "Viscous Hypersonic Flow Over Complex Bodies at High Angles of Attack," AIAA Paper 84-0015, January 1984.